IEEE Access
Multidisciplinary | Rapid Review | Open Access Journal

Received January 11, 2020, accepted January 22, 2020, date of publication January 27, 2020, date of current version February 10, 2020.

Digital Object Identifier 10.1109/ACCESS.2020.2969778

A Highly Efficient Spectrum Sensing Approach Based on Antenna Arrays Beamforming

AMR HUSSEIN HUSSEIN[1], HAGER SHAWKY FOUDA[1], HAYTHEM HUSSEIN ABDULLAH[2], AND ASHRAF A. M. KHALAF[3]

[1]Electronics and Electrical Communications Engineering Department, Faculty of Engineering, Tanta University, Tanta 31111, Egypt
[2]Electronics Research Institute, Giza 12622, Egypt
[3]Electronics and Communications Department, Faculty of Engineering, Minia University, Minia 61519, Egypt

Corresponding author: Haythem Hussein Abdullah (haythm_eri@yahoo.com)

ABSTRACT In cognitive radio (CR), the sensitivity of the spectrum sensing (SS) algorithms depends mainly on several factors such as the receiver sensitivity, the antenna gain, the antenna efficiency and the SS algorithm itself. Researchers depend mainly on a single antenna element and sometimes on a uniform linear antenna (ULA) arrays to increase the system sensitivity. But actually the ULA suffers from the large side lobe level which in turn reduces the antenna gain. Furthermore, the separation between elements in the ULA is almost chosen to be half wavelength at the operating frequency which results in a dense array of close elements. If this separation increases slightly in order to reduce the mutual coupling between elements, the side lobes will increase and thus the realized gain is reduced more and more and as a consequence, the SNR will be reduced also which has a direct effect on the sensitivity of the system. In this paper, a low complexity and highly efficient SS technique based on antenna arrays beamforming and the generalized likelihood ratio test (GLRT) denoted as BF/GD is introduced. The proposed beamforming approach allows the utilization of the limited number of ULA elements and their corresponding RF chains to synthesize the desired radiation patterns of larger size antenna arrays for maximum gain realization. The desired pattern is realized by optimizing the excitation coefficients and inter-element spacing of the array. Consequently, the enhancement in the realized array gain will lead to a direct increase in the received signal-to-noise ratio (SNR) which significantly improves the sensitivity and the SS capability of the CR receiver without the need for extra hardware.

INDEX TERMS Beamforming (BF), cognitive radio (CR), spectrum sensing (SS), multiple antenna elements (MAE), uniform linear array (ULA), generalized likelihood ratio test (GLRT).

I. INTRODUCTION

In this section, an introduction to CR communications and recent techniques used to improve the performance of the SS algorithms is presented. Next is an introduction to digital antenna arrays beamforming techniques and how to apply them to CR systems to improve their detection performance. Firstly, the wireless communication capacity has reached the saturation level and this has been exacerbated by the emergence of greedy bandwidth applications. CR communication is one of the most promising technologies in the wireless communication field, because of its superior ability to solve the problem of bandwidth shortage caused by services requiring broadband. This technology permits efficient spectral collaboration between the unlicensed secondary users (SU) and the underlying licensed primary users (PU) without affecting the performance of these users [1], [2]. This type of coexistence requires the SU to continuously and separately monitor the presence of the PU. This process is known as spectrum sensing (SS), which is the basis for the construction of any CR system. In this case, the temporary unused spectrum holes will be used efficiently by the SU until the PU returns to use his licensed frequency band [3]. Effective research efforts have been exerted in this area and many SS techniques have been introduced for efficient utilization of the limited frequency resources [4]–[10]. One of the most popular SS technologies is the energy detector (ED), which is characterized by its low complexity and the lack of prior knowledge of the PU signal parameters and channel characteristics. But its performance worsens as the SNR decreases.

The associate editor coordinating the review of this manuscript and approving it for publication was Yingsong Li.

Also, it compares the signal energy to the estimated noise variance, which is affected by the noise uncertainty problems [4], [5]. To overcome these problems, several SS algorithms based on eigenvalue decomposition of the received signal covariance matrix are introduced in [6]–[9]. The covariance matrix is formed from the received signals incident on the multiple antenna elements (MAE) of the CR receiver. The maximum and minimum eigenvalues of the signal covariance matrix are efficiently used to decide the presence/ absence of the PU signal. In [6], the Maximum-Minimum Eigenvalue (MME) SS technique has utilized the ratio of the maximum eigenvalue to the minimum eigenvalue as a test statistic for PU detection. In the same paper, the Energy with Minimum Eigenvalue (EME) SS algorithm is also introduced using the ratio of the calculated signal energy to the minimum eigenvalue as a test statistic. In [7], the signal to noise eigenvalue (SNE) based SS algorithm is introduced for a single PU detection. While in [8], the Arithmetic to Geometric Mean (AGM) algorithm has employed the ratio of the arithmetic mean to the geometric mean of the eigenvalues as a test statistic. In [9], two high-performance volume-based detection algorithms denoted as VD1 and VD2 are introduced where their test statistics are also based on the eigenvalue decomposition of the covariance matrix. In [10], a Generalized Likelihood Ratio Test/ Direction of Arrival estimation (GD) based SS algorithm was introduced. In this algorithm, in order to take the advantage of the receiving ULA gain, delay and sum beamforming was performed to combine the received PU signal versions constructively considering the random nature of the noise signals at each antenna element.

Secondly, it is worth noting that the utilization of MAE or antenna arrays has significant importance in many applications such as satellite communications, radar systems, mobile communications, and CR systems. The use of a large number of antenna elements at the CR base stations are preferred for reliable communications. While a large number of antenna elements at the CR terminals is typically avoided due to the constraints on the terminal size, weight, and deployment complexity.

Antenna arrays beamforming can be considered as one of the most promising solutions that can solve these constraints on communication systems as well as its ability to significantly improve their performance. Beamforming can be defined as the process in which the radiation pattern of an antenna array is shaped according to certain optimum criteria. These criteria could be maximizing the signal-to-interference ratio (SIR), steering the main beam towards a signal of interest, nulling the interfering signals, side lobe level (SLL) reduction, and tracking a moving emitter to name a few [11]–[13]. To solve the limited array size restriction on the CR terminals, many beamforming research efforts are attempted to synthesize large size linear antenna arrays using a reduced number of antenna elements [14]–[22]. Several analytical algorithms based on the matrix pencil method (MPM) and the forward-backward matrix pencil method (FBMPM) are introduced in [14], [15]. These algorithms provide accurate arrays synthesis by controling both the elements excitations and spacings. On the other hand, several optimization-based array beamforming algorithms were introduced to solve the typically complicated radiation pattern synthesis problems of the analytical techniques. These algorithms include vector Tabu search (VTS), simulated annealing (SA), genetic algorithm (GA), particle swarm optimization (PSO), and differential evolution algorithms (DEA) [16]–[20]. The common target of these algorithms is the search for the optimum solutions of the element's excitations (magnitude and phase) and inter-elements spacing required to synthesize the desired array pattern. But they are time consuming methods especially for large size and shaped pattern arrays. To avoid the excessive search burden of the optimization-based techniques, new hybrid algorithms based on a combination between analytical and optimization algorithms are introduced in [21], [22]. In [21], a hybrid technique between the method of moments (MoM) and the genetic algorithm, (MoM/GA), was introduced for linear antenna arrays synthesis using a fewer number of antenna elements using either uniform or non-uniform element spacing that are determined using the GA. While the MoM provides a deterministic solution for the corresponding excitation coefficients. In [22], an efficient array synthesis algorithm based on a combination between the Fast Fourier Transform (FFT), Curve Fitting (CF), and the GA denoted as FFT/CF/GA was introduced. It also provides a reduction in the number of elements using either a uniform or non-uniform element spacing. The FFT of the desired array pattern is used to determine the excitation coefficients of the array elements. The curve fitting technique is used to generate a fitting polynomial that relates the predetermined excitation coefficients using FFT to the corresponding optimized elements positions. The aforementioned fixed beamforming techniques have attractive performances in the case of non-sparse antenna arrays. However, many adaptive beamforming algorithms for sparse antenna arrays are introduced. Recently, an efficient adaptive sparse beamforming algorithm named as L_0-norm constrained normalized least-mean-square (L_0-CNLMS) is introduced in [23]. The L_0-CNLMS achieved excellent beamforming for different arrays sizes, configurations, and conditions using fewer number of antenna elements compared to the adaptive sparse beamforming algorithms such as the L1-norm linearly constrained normalized least-mean-square (L_1-CNLMS) algorithm and its weighted version (L_1-WCNLMS) introduced in [24]. As the approximate L_0-norm constrained algorithm provides faster convergence than the L_1-norm constrained algorithm, it is widely used in sparse beamforming and direction of arrival (DOA) estimation algorithms as introduced in [24].

In this paper, low complexity and highly efficient SS technique based on fixed antenna arrays beamforming and the GLRT denoted as (BF/GD) is introduced. The proposed beamforming allows the utilization of the limited number of ULA elements of the CR terminal to synthesize the radiation pattern of a desired larger-size antenna array for maximum

array gain realization. The desired pattern is obtained by the optimization of the elements spacing and excitations. As a result, increasing the array gain will increase the received SNR which significantly improves the sensitivity and the SS capability of the CR receiver. The derivations of the proposed array beamforming approach, the proposed signal model, and the test statistic of the proposed BF/GD technique are introduced. Several simulations are carried out to verify the effectiveness and the superiority of the proposed BF/GD technique compared to the traditional ULA based SS techniques such as GD, AGM, MME, SNE, VD1, VD2, and ED. Furthermore, when the proposed signal model is applied to the aforementioned techniques, significant improvements in their performances are achieved. Accordingly, they are renamed as BF/AGM, BF/MME, BF/SNE, BF/VD1, BF/VD2, and BF/ED, respectively in order to differentiate them before and after the application of the proposed antenna array beamforming.

The rest of the paper is organized as follows. In Section II, the general signal model of the ULA based CR system is presented. The clarification of the problem formulation is introduced in Section III. The proposed antenna array beamforming technique and the proposed signal model are introduced in Section IV. The proposed beamforming based GD algorithm (BF/GD) and its test statistic are illustrated in Section V. In Section VI, the simulation results of array beamforming and SS algorithms are discussed. Finally, the paper is concluded in Section VII.

II. GENERAL SIGNAL MODEL OF THE ULA BASED CR SYSTEMS

Consider a MAE based CR receiver utilizing a ULA consisting of M antenna elements with uniform element spacing $d = \lambda/2$. Where λ is the wavelength of the received narrow band PU signal. The ULA array factor $A_f(\theta)$ is given by [21]

$$A_f(\theta) = \sum_{m=1}^{M} a_m e^{i\beta(m-1)d\cos\theta} \tag{1}$$

where a_m is the excitation coefficient of the m^{th} antenna element such that $a_m = 1$ for ULA. $\beta = 2\pi/\lambda$ is the free space wave number. Consider a single PU signal impinging on the receiving antenna array from a known direction θ_{PU}, then the array steering vector A is given by:

$$\boldsymbol{A} = A_f(\theta_{PU}) \tag{2}$$

$$\boldsymbol{A} = [1 e^{j\beta d\cos(\theta_{PU})} e^{j2\beta d\cos(\theta_{PU})} \ldots e^{j(M-1)\beta d\cos(\theta_{PU})}]^T \tag{3}$$

where $[.]^T$ is the transpose operator. The received signal $\boldsymbol{y}(n)$ can be written as:

$$\boldsymbol{y}(n) = \boldsymbol{A}s(n) + \boldsymbol{w}(n), \quad n = 1, 2, \ldots, N \tag{4}$$

where N is the number of received signal samples, $s(n)$ is the PU transmitted signal, $\boldsymbol{w}(n)$ is a complex white Gaussian noise (CWGN) with zero mean $\mu_w = 0$ and variance σ_w^2. $\boldsymbol{y}(n)$ and $\boldsymbol{w}(n)$ can be expressed in a matrix form as follows:

$$\boldsymbol{y}(n) = \begin{bmatrix} y_1(n) & y_2(n) & \ldots & y_M(n) \end{bmatrix}^T \tag{5}$$

$$\boldsymbol{w}(n) = \begin{bmatrix} w_1(n) & w_2(n) & \ldots & w_M(n) \end{bmatrix}^T \tag{6}$$

Define $\mathcal{H}_0$ and $\mathcal{H}_1$ as the signal-absence and signal-presence hypotheses, respectively. The received signal $\boldsymbol{y}(n)$ under these hypotheses can be expressed as:

$$\boldsymbol{y}(n) = \begin{cases} \boldsymbol{w}(n), & \mathcal{H}_0 \\ \boldsymbol{A}s(n) + \boldsymbol{w}(n), & \mathcal{H}_1 \end{cases} \tag{7}$$

III. PROBLEM FORMULATION

The traditional CR systems employ ULAs of limited sizes and gains at the CR receiving terminals to avoid excessive weight, size, and complexity. These restrictions limit the received SNR and SS capability of the system. As a solution, beamforming of antenna arrays for maximum gain realization can significantly mitigate these limitations. By applying beamforming technique, the M limited number of antenna elements of the traditional ULA are used to synthesize the array pattern of larger size M_L-elements antenna arrays, $M_L > M$, by optimizing the elements spacing and excitation coefficients. The synthesized array pattern using the M elements will have approximately the same array gain, half power beamwidth (HPBW), and side lobe level (SLL) of the M_L-elements antenna array. Consequently, higher array gain is realized without using additional antenna elements. Moreover, the SNR of the received signal will be increased in proportion to the gain increment. As a result, significant performance enhancement of the MAE based SS techniques will be achieved. Another parameter that significantly affects the performance of the CR system is the SS time that should be as small as possible for efficient spectrum utilization. In our case, the beamforming will allow higher SS performance using a minimum number of antenna elements which reduces the number of received signal samples, required storage, system complexity, signal processing, and the SS time.

IV. PROPOSED ANTENNA ARRAY BEAMFORMING TECHNIQUE AND MODIFIED RECEIVED SIGNAL MODEL

The MoM/GA array beamforming technique introduced in [21] is selected due to its attractive features compared to the aforementioned beamforming techniques which can be summarized as follows: (a) The MPM and FBMPM provide an ill-conditioned matrix that requires special treatment using singular value decomposition (SVD) technique. Also, they have high computational complexity, (b) the optimization techniques are based on finding the solution of many unknown parameters such as the excitation amplitudes and phases and the location of each element. These optimization techniques provide good results but they are time-consuming, (c) The MoM/GA uses a simple matrix inversion algorithm, (d) the MoM/GA does not suffer from the existence of the complex element spacing values that are unrealizable as in case of the appearance of high imaginary parts as in the MPM and the FBMPM algorithms, and (e) the MoM/GA is also characterized by fast convergence, high accuracy, less computational complexity compared to other methods such as Marcano's GA based algorithm, MPM, and FBMPM. Finally,

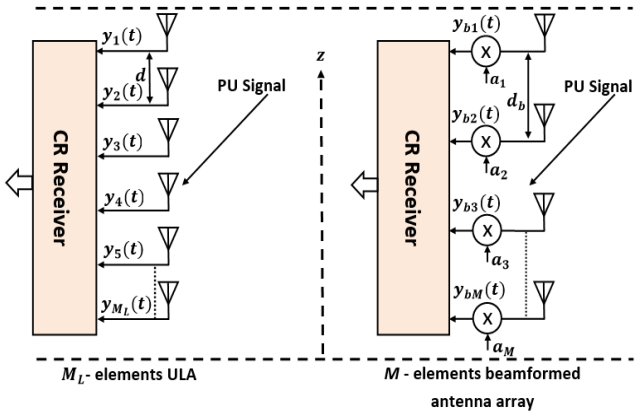

FIGURE 1. The CR receiver using beamformed M-elements antenna array compared to the CR receiver using M_L-elements ULA where $M < M_L$.

it can be used for array synthesis using uniform and non-uniform element spacing.

In this work, unlike what was mentioned in [21] that the MoM/GA is used to synthesize the antenna arrays using reduced number of antenna elements, the MoM/GA algorithm has been modified so that it can use the few available antenna elements to synthesize the radiation patterns of larger size antenna arrays.

Consider a MAE based CR receiver equipped with M-elements ULA with uniform element spacing d. It is required to utilize the existing M antenna elements to synthesize the radiation pattern of the desired M_L-elements ULA such that $M < M_L$ as shown in Fig. 1.

According to (1), the array factor of the desired ULA, $A_{fd}(\theta)$, can be expressed as:

$$A_{fd}(\theta) = \sum_{l=1}^{M_L} a_l e^{i\beta(l-1)d\cos\theta} \tag{8}$$

where a_l is the excitation coefficient of the l^{th} antenna element of the desired ULA and $a_l = 1$ for $l = 1, 2, 3, \ldots, M_L$.

The array factor $A_{fs}(\theta)$ of the synthesized array should be coincided with the desired array factor $A_{fd}(\theta)$ which can be expressed as follows:

$$A_{fs}(\theta) \approx A_{fd}(\theta) \tag{9}$$

$$\sum_{b=1}^{M} a_b e^{j\beta(b-1)d_b\cos\theta} \approx \sum_{l=1}^{M_L} a_l e^{i\beta(l-1)d\cos\theta} \tag{10}$$

where a_b and d_b are the synthesized excitation coefficient and element spacing of the synthesized array, respectively. Let Q is the number of samples required to represent the desired array pattern such that:

$$A_{fd}(\boldsymbol{\theta}) = [A_{fd}(\theta_1) A_{fd}(\theta_2) A_{fd}(\theta_3) \ldots\ldots A_{fd}(\theta_Q)] \tag{11}$$

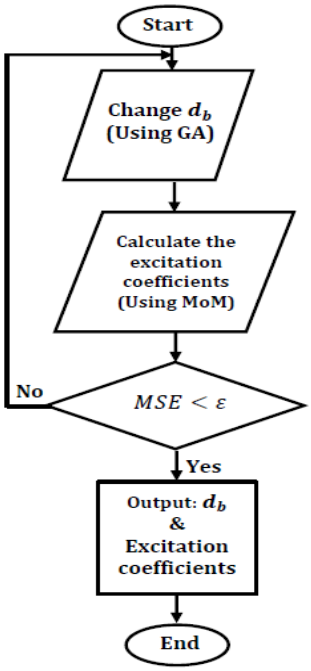

FIGURE 2. The flowchart of the proposed array synthesis technique.

where $\boldsymbol{\theta} = [\theta_1, \theta_2, \theta_3, \ldots\ldots, \theta_Q]$ are the sample angles such that $0 \le \theta_q \le 2\pi$ and $q = 1, 2, 3, \ldots, Q$. Then (10) can be written in a matrix form as follows (12), as shown at the bottom of this page.

Let $[\mathbb{C}]_{1\times M}$, $[\mathbb{Q}]_{M\times Q}$, and $[\mathbb{R}]_{1\times Q}$, as shown at the bottom of the next page. Then (12) can be simplified to

$$[\mathbb{C}]_{1\times M}[\mathbb{Q}]_{M\times Q} = [\mathbb{R}]_{1\times Q} \tag{13}$$

It is required to solve (13) to determine the optimum element spacing d_b and the excitation coefficients vector $[\mathbb{C}]_{1\times M}$. Multiply both sides of (13) by $[\mathbb{Q}]^H_{M\times Q}$ which is defined as the hermitian transpose of the matrix $[\mathbb{Q}]_{M\times Q}$ then

$$[\mathbb{C}]_{1\times M}[\mathbb{Q}]_{M\times Q}[\mathbb{Q}]^H_{M\times Q} = [\mathbb{R}]_{1\times Q}[\mathbb{Q}]^H_{M\times Q} \tag{14}$$

Let $[\mathbb{R}_{\boldsymbol{QQ}}]_{M\times M} = [\mathbb{Q}]_{M\times Q}[\mathbb{Q}]^H_{M\times Q}$, then (14) is rewritten as:

$$[\mathbb{C}]_{1\times M}[\mathbb{R}_{\boldsymbol{QQ}}]_{M\times M} = [\mathbb{R}]_{1\times Q}[\mathbb{Q}]^H_{M\times Q} \tag{15}$$

The excitation coefficients $[\mathbb{C}]_{1\times M}$ can be obtained as:

$$[\mathbb{C}]_{1\times M} = [\mathbb{R}]_{1\times Q}[\mathbb{Q}]^H_{M\times Q}[\mathbb{R}_{\boldsymbol{QQ}}]^{-1}_{M\times M} \tag{16}$$

where $[\mathbb{R}_{\boldsymbol{QQ}}]^{-1}_{M\times M}$ is the inverse of the matrix $[\mathbb{R}_{\boldsymbol{QQ}}]_{M\times M}$.

$$[a_1 a_2 \ldots\ldots a_M] \times \begin{bmatrix} 1 & 1 & \ldots & 1 \\ e^{j\beta d_b\cos\theta_1} & e^{j\beta d_b\cos\theta_2} & \ldots & e^{j\beta d_b\cos\theta_Q} \\ \ldots & \ldots & \ldots & \ldots \\ e^{j(M-1)\beta d_b\cos\theta_1} & e^{j(M-1)\beta d_b\cos\theta_2} & \ldots & e^{j(M-1)\beta d_b\cos\theta_Q} \end{bmatrix} = [A_{fd}(\theta_1) A_{fd}(\theta_1) A_{fd}(\theta_1) \ldots\ldots A_{fd}(\theta_Q)] \tag{12}$$

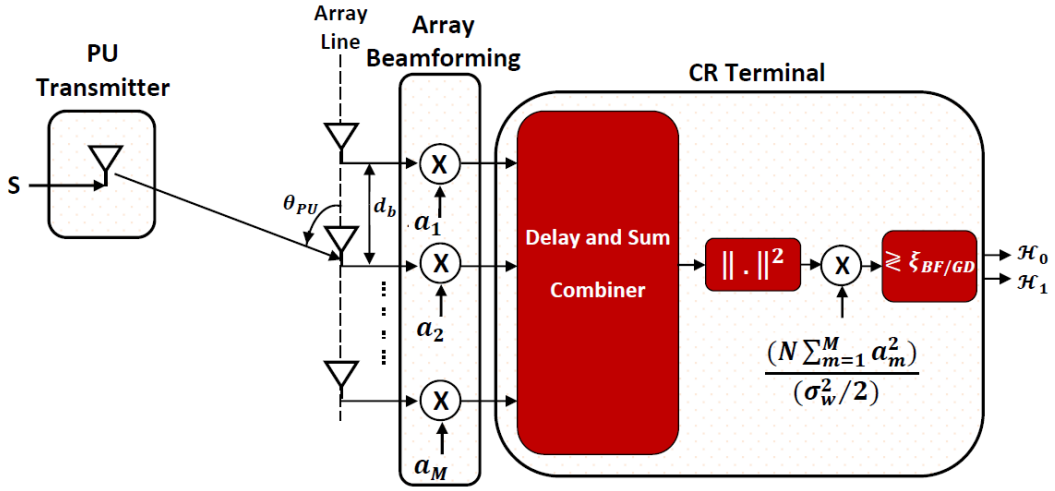

FIGURE 3. The block diagram of the proposed BF/GD algorithm.

But, (16) has two unknown parameters d_b and $[\mathbb{C}]_{1\times M}$ which makes it difficult to solve this equation by the traditional techniques. This equation can be solved using the GA optimization tool to determine the optimal element spacing d_b as it is confined within a specific range $\lambda/2 \leq d_b < \lambda$. For a given value of the parameter d_b, the excitation coefficients vector $[\mathbb{C}]_{1\times M}$ are simply obtained from (16). The GA searches for the optimum value of the element spacing d_b to minimize the designed cost function which is represented as the summation of the mean square errors between the desired and synthesized patterns and their half power beamwidths. The flow of the algorithm is depicted in the flowchart of Fig. 2. Where MSE is the mean square error and ε is the MSE threshold which is set to 0.001.

$$= \left\{ \frac{\sum_{q=1}^{Q} \left\| A_{fs}\left(\theta_q\right) - A_{fd}\left(\theta_q\right) \right\|^2}{Q} + \| HPBW_s - HPBW_d \|^2 \right\} \tag{17}$$

where $HPBW_s$ and $HPBW_d$ are the half power beamwidth of the synthesized and desired patterns, respectively.

Now to obtain the proposed beamforming-based signal model, consider a single PU signal impinging on the receiving antenna array from a known direction θ_{PU}, then the steering vector $\boldsymbol{A_b}$ of the beamformed antenna array is given by:

$$\boldsymbol{A_b} = A_{fs}(\theta_{PU}) \tag{18}$$

$$\boldsymbol{A_b} = \begin{bmatrix} a_1 & a_2 e^{j\beta d_b \cos(\theta_{PU})} & a_3 e^{j2\beta d_b \cos(\theta_{PU})} \\ \cdots & a_M e^{j(M-1)\beta d_b \cos(\theta_{PU})} \end{bmatrix}^T \tag{19}$$

In this case, the modified beamforming based received signal model $\boldsymbol{y_b}(n)$ can be written as:

$$\boldsymbol{y_b}(n) = \boldsymbol{A_b} s(n) + \boldsymbol{w}(n), \quad n = 1, 2, \ldots, N \tag{20}$$

V. PROPOSED BEAMFORMING BASED GD ALGORITHM (BF/GD)

In this section, the proposed array beamforming is applied to GD SS algorithm introduced in [10]. The block diagram of the proposed BF/GD algorithm is shown in Fig. 3. Using the same narrow band signal model introduced in [10], $s(n) = A_m e^{j2\pi n f_0 + \varphi}$ where A_m and φ are the signal amplitude and phase, respectively. $f_0 \leq 0.5$ is the normalized frequency. Then (20) can be rewritten as:

$$\boldsymbol{y_b}(n) = \boldsymbol{A_b}(A_m e^{j2\pi n f_0 + \varphi}) + \boldsymbol{w}(n), \; n = 1, 2, \ldots, N \tag{21}$$

In order to apply the GLRT simplified linear model [10], the beamformed signal in (21) is rearranged in a temporal order, $\boldsymbol{y_{bt}}(k)$, where the received signal becomes $MN \times 1$ large

$$[\mathbb{C}]_{1\times M} = [a_1 a_2 \ldots\ldots a_M]$$

$$[\mathbb{Q}]_{M\times Q} = \begin{bmatrix} 1 & 1 & \cdots & 1 \\ e^{j\beta d_b \cos\theta_1} & e^{j\beta d_b \cos\theta_2} & \cdots & e^{j\beta d_b \cos\theta_Q} \\ \cdots & \cdots & \cdots & \cdots \\ e^{j(M-1)\beta d_b \cos\theta_1} & e^{j(M-1)\beta d_b \cos\theta_2} & \cdots & e^{j(M-1)\beta d_b \cos\theta_Q} \end{bmatrix}$$

$$[\mathbb{R}]_{1\times Q} = A_{fd}(\boldsymbol{\theta}) = [A_{fd}(\theta_1) A_{fd}(\theta_2) A_{fd}(\theta_3) \ldots\ldots A_{fd}(\theta_Q)]$$

column vector [10]. Thus, the received signal $\boldsymbol{y_{bt}}(k)$ can be rewritten as:

$$\boldsymbol{y_{bt}}(k) = \underbrace{\begin{bmatrix} a_{11}e^{j2\pi f_0} \\ a_{21}e^{j(2\pi f_0+\beta d_b\cos(\theta_{PU}))} \\ a_{M1}e^{j(2\pi f_0+(M-1)\beta d_b\cos(\theta_{PU}))} \\ \cdots \\ \cdots \\ a_{1N}e^{j2\pi Nf_o} \\ a_{2N}e^{j(2\pi Nf_0+\beta d_b\cos(\theta_{PU}))} \\ \vdots \\ a_{MN}e^{j(2\pi Nf_0+(M-1)\beta d_b\cos(\theta_{PU}))} \end{bmatrix}}_{\boldsymbol{\Omega}=\boldsymbol{A_t}\boldsymbol{\Phi}} A_m e^{j\varphi} + \begin{bmatrix} w_{11}(1) \\ w_{21}(1) \\ \vdots \\ w_{M1}(1) \\ \cdots \\ \cdots \\ w_{1N}(N) \\ w_{2N}(N) \\ \vdots \\ w_{MN}(N) \end{bmatrix} \quad (22)$$

Let $\boldsymbol{A_t} = diag(a_{11}a_{21}\ldots a_{M1}a_{12}a_{22}\ldots a_{M2}\ldots a_{1N}a_{2N}\ldots a_{MN})$ is the $MN \times MN$ beamformed array excitation coefficients matrix whose diagonal elements can be expressed as:

$$a_{mn} = a_m \forall m = 1, 2, \ldots .M \text{ and } n = 1, 2, \ldots .N \quad (23)$$

$\Phi_{mn} = e^{(2\pi nf_0+\beta(m-1)d_b\cos(\theta_{PU}))}$ is the element of the $MN \times 1$ matrix $\boldsymbol{\Phi}$. $\boldsymbol{\Omega} = \boldsymbol{A_t}\boldsymbol{\Phi}$ is the $MN \times 1$ known observation matrix. And $\Psi = A_m e^{j\varphi}$ is the unknown signal parameter. $\boldsymbol{w_t}(k)$ is the temporal ordered $MN \times 1$ noise vector. Then (22) can be expressed as:

$$\boldsymbol{y_{bt}}(k) = \boldsymbol{\Omega\Psi} + \boldsymbol{w_t}(k), \quad k = 1, 2, 3, \ldots .MN \quad (24)$$

For the temporal ordered signal $\boldsymbol{y_{bt}}(k)$, the binary hypotheses can be expressed as:

$$\boldsymbol{y_{bt}}(k) = \begin{cases} \boldsymbol{w_t}(k), & \mathcal{H}_0 \\ \boldsymbol{\Omega\Psi} + \boldsymbol{w_t}(k), & \mathcal{H}_1 \end{cases} \quad (25)$$

A. DERIVATION OF THE TEST STATISTIC

In this section, the test statistic of the proposed algorithm is derived considering the prior knowledge of the noise variance. The generalized likelihood ratio test (GLRT) is defined as [10]:

$$T(\boldsymbol{y_{bt}}) = \frac{p\left(\boldsymbol{y_{bt}} \mid \mathcal{H}_1; \hat{\Psi}_1\right)}{p\left(\boldsymbol{y_{bt}} \mid \mathcal{H}_0; \hat{\Psi}_0\right)} \underset{\mathcal{H}_1}{\overset{\mathcal{H}_0}{\lessgtr}} \xi \quad (26)$$

where ξ is the threshold. $\hat{\Psi}_1$ and $\hat{\Psi}_0$ are the set of unknown PU signal parameters under the two hypotheses $\mathcal{H}_1$ and $\mathcal{H}$, respectively. The maximum likelihood estimates of these parameters are defined as:

$$\hat{\Psi}_0 = \frac{\arg max}{\Psi_0} p\left(\boldsymbol{y_{bt}} \mid \mathcal{H}_0; \Psi_0\right) \quad (27)$$

$$\hat{\Psi}_1 = \frac{\arg max}{\Psi_1} p\left(\boldsymbol{y_{bt}} \mid \mathcal{H}_1; \Psi_1\right) \quad (28)$$

B. PROOF

By applying the GLRT simplified linear model [10] on the modified signal model, the BF/GD test statistic is given by:

$$T_{BF/GD(\sigma_w^2)}(\boldsymbol{y_{bt}}) = \frac{1}{\sigma_w^2/2}\boldsymbol{y_{bt}}^H \boldsymbol{\Omega}(\boldsymbol{\Omega}^H\boldsymbol{\Omega})^{-1}\boldsymbol{\Omega}^H\boldsymbol{y_{bt}} \underset{\mathcal{H}_0}{\overset{\mathcal{H}_1}{\lessgtr}} \xi_{BF/GD(\sigma_w^2)} \quad (29)$$

The term $(\boldsymbol{\Omega}^H\boldsymbol{\Omega})^{-1}$ can be calculated as

$$(\boldsymbol{\Omega}^H\boldsymbol{\Omega})^{-1} = (\boldsymbol{\Phi}^H\boldsymbol{A_t}^H\boldsymbol{A_t}\boldsymbol{\Phi})^{-1} \quad (30)$$

For real excitation coefficients, Eq. (30) can be rewritten as

$$(\boldsymbol{\Omega}^H\boldsymbol{\Omega})^{-1} = (\boldsymbol{\Phi}^H\boldsymbol{A_t}^H\boldsymbol{A_t}\boldsymbol{\Phi})^{-1} = (N\sum_{m=1}^{M} a_m^2)^{-1} \quad (31)$$

It is clear that $(\boldsymbol{\Omega}^H\boldsymbol{\Omega})^{-1}$ is a scalar and in this case, (29) is expressed as follows:

$$T_{BF/GD(\sigma_w^2)}(\boldsymbol{y_{bt}}) = \frac{1}{(\sigma_w^2/2)(N\sum_{m=1}^{M} a_m^2)}(\boldsymbol{y_{bt}}^H\boldsymbol{\Omega}\boldsymbol{\Omega}^H\boldsymbol{y_{bt}}) \underset{\mathcal{H}_0}{\overset{\mathcal{H}_1}{\lessgtr}} \xi_{BF/GD(\sigma_w^2)} \quad (32)$$

As $\left(\boldsymbol{y_{bt}}^H\boldsymbol{\Omega}\boldsymbol{\Omega}^H\boldsymbol{y_{bt}}\right) = \left\|\boldsymbol{\Omega}^H\boldsymbol{y_{bt}}\right\|^2$, then

$$T_{BF/GD(\sigma_w^2)}(\boldsymbol{y_{bt}}) = \frac{1}{(\sigma_w^2/2)(N\sum_{m=1}^{M} a_m^2)}\left\|\boldsymbol{\Omega}^H\boldsymbol{y_{bt}}\right\|^2 \underset{\mathcal{H}_0}{\overset{\mathcal{H}_1}{\lessgtr}} \xi_{BF/GD(\sigma_w^2)} \quad (33)$$

$\left\|\boldsymbol{\Omega}^H\boldsymbol{y_{bt}}\right\|^2$ is the power of the temporal ordered $MN \times 1$ co-phased received signal vector which is the same as the power obtained from the $M \times N$ co-phased received signal matrix which is given by:

$$\left\|\boldsymbol{\Omega}^H\boldsymbol{y_{bt}}\right\|^2 = \left\|\boldsymbol{\Omega}^H(\boldsymbol{\Omega\Psi} + \boldsymbol{w_t}(k))\right\|^2 = \left\|\boldsymbol{\Omega}^H\boldsymbol{\Omega\Psi} + \boldsymbol{\Omega}^H\boldsymbol{w_t}(k)\right\|^2 \quad (34)$$

Substituting $\boldsymbol{\Omega}^H\boldsymbol{\Omega} = N\sum_{m=1}^{M} a_m^2$ from (31), then (34) can be rewritten as

$$\left\|\boldsymbol{\Omega}^H\boldsymbol{y_{bt}}\right\|^2 = \left\|\left(N\sum_{m=1}^{M} a_m^2\right)\Psi + \boldsymbol{\Omega}^H\boldsymbol{w_t}(k)\right\|^2 \quad (35)$$

Substituting (35) in (33), the test statistic is expressed as

$$T_{BF/GD(\sigma_w^2)}(\boldsymbol{y_{bt}}) = \frac{1}{(\sigma_w^2/2)(N\sum_{m=1}^{M} a_m^2)} \times \left\|\left(N\sum_{m=1}^{M} a_m^2\right)\Psi + \boldsymbol{\Omega}^H\boldsymbol{w_t}(k)\right\|^2 \underset{\mathcal{H}_1}{\overset{\mathcal{H}_0}{\lessgtr}} \xi_{BF/GD(\sigma_w^2)} \quad (36)$$

By multiplying (36) by $\frac{(N\sum_{m=1}^{M}a_m^2)}{(N\sum_{m=1}^{M}a_m^2)}$, the $T_{BF/GD(\sigma_w^2)}$ can be expressed as:

$$\begin{aligned}
&T_{BF/GD(\sigma_w^2)}\left(\boldsymbol{y_{bt}}\right)\\
&=\frac{(N\sum_{m=1}^{M}a_m^2)}{(\sigma_w^2/2)(N\sum_{m=1}^{M}a_m^2)^2}\\
&\quad\times\left\|\left(N\sum_{m=1}^{M}a_m^2\right)\Psi+\boldsymbol{\Omega}^H\boldsymbol{w_t}(k)\right\|^2\underset{\mathcal{H}_1}{\overset{\mathcal{H}_0}{\lessgtr}}\xi_{BF/GD(\sigma_w^2)}\\
&=\frac{(N\sum_{m=1}^{M}a_m^2)}{(\sigma_w^2/2)}\\
&\quad\times\left\|\frac{\left(N\sum_{m=1}^{M}a_m^2\right)\Psi}{(N\sum_{m=1}^{M}a_m^2)}+\frac{\boldsymbol{\Omega}^H\boldsymbol{w_t}(k)}{(N\sum_{m=1}^{M}a_m^2)}\right\|^2\underset{\mathcal{H}_1}{\overset{\mathcal{H}_0}{\lessgtr}}\xi_{BF/GD(\sigma_w^2)}\\
&=\frac{(N\sum_{m=1}^{M}a_m^2)}{(\sigma_w^2/2)}\left\|\Psi+\frac{\boldsymbol{\Omega}^H\boldsymbol{w_t}(k)}{(N\sum_{m=1}^{M}a_m^2)}\right\|^2\underset{\mathcal{H}_1}{\overset{\mathcal{H}_0}{\lessgtr}}\xi_{BF/GD(\sigma_w^2)}
\end{aligned}\tag{37}$$

From (37), the first term Ψ illustrates that the delay and sum combiner succeeded to detect the PU signal. While the second term $\frac{\boldsymbol{\Omega}^H\boldsymbol{w_t}(k)}{(N\sum_{m=1}^{M}a_m^2)}$ represents the destructively combined noise.

C. TEST STATISTIC UNDER UNKNOWN NOISE POWER CONDITION

In practical CR networks, the true value of the noise variance σ_w^2 cannot be determined. From this respect, the estimated value of the noise variance $\hat{\sigma}_w^2$ should be calculated instead. In general, the maximum likelihood estimation of the noise variance $\hat{\sigma}_w^2$ under $\mathcal{H}_1$ can be expressed as [26]

$$\hat{\sigma}_w^2=\frac{1}{N_r-df}\boldsymbol{y}^H(\boldsymbol{I}-\boldsymbol{\Omega}\left(\boldsymbol{\Omega}^H\boldsymbol{\Omega}\right)^{-1}\boldsymbol{\Omega}^H)\boldsymbol{y}\tag{38}$$

where N_r is the number of data records, df is the degree of freedom of the matrix $\boldsymbol{\Omega}$, $\boldsymbol{I}$ is $N_r\times N_r$ identity matrix, and $\boldsymbol{y}$ is the received signal. For the proposed beamforming based signal model, these parameters and variables are set to $N_r=MN$ and $\boldsymbol{y}=\boldsymbol{y_{bt}}$. For a single PU transmitting a complex signal $s(n)$ consisting of two parts: real and imaginary, the degree of freedom parameter is set to $df=2$. By substituting these parameters and variables in (38), the $\hat{\sigma}_w^2$ can be rewritten as:

$$\hat{\sigma}_w^2=\frac{1}{MN-2}\boldsymbol{y_{bt}}^H\left(\boldsymbol{I}-\boldsymbol{\Omega}(\boldsymbol{\Omega}^H\boldsymbol{\Omega})^{-1}\boldsymbol{\Omega}^H\right)\boldsymbol{y_{bt}}\tag{39}$$

From the GLRT simplified linear model for unknown noise variance, the test statistic is given by:

$$\begin{aligned}
&T_{BF/GD(\hat{\sigma}_w^2)}\left(\boldsymbol{y_{bt}}\right)\\
&\quad=\frac{1}{\hat{\sigma}_w^2/2}\boldsymbol{y_{bt}}^H\boldsymbol{\Omega}(\boldsymbol{\Omega}^H\boldsymbol{\Omega})^{-1}\boldsymbol{\Omega}^H\boldsymbol{y_{bt}}\underset{\mathcal{H}_0}{\overset{\mathcal{H}_1}{\lessgtr}}\xi_{BF/GD(\hat{\sigma}_w^2)}
\end{aligned}\tag{40}$$

Substituting the value of $\hat{\sigma}_w^2$ given by (39) in (40), the test statistic can be rewritten as

$$\begin{aligned}
&T_{BF/GD(\hat{\sigma}_w^2)}\left(\boldsymbol{y_{bt}}\right)\\
&\quad=\frac{2\,(MN-2)}{2}\\
&\qquad\times\frac{\boldsymbol{y_{bt}}^H\boldsymbol{\Omega}(\boldsymbol{\Omega}^H\boldsymbol{\Omega})^{-1}\boldsymbol{\Omega}^H\boldsymbol{y_{bt}}}{\boldsymbol{y_{bt}}^H\left(\boldsymbol{I}-\boldsymbol{\Omega}(\boldsymbol{\Omega}^H\boldsymbol{\Omega})^{-1}\boldsymbol{\Omega}^H\right)\boldsymbol{y_{bt}}}\underset{\mathcal{H}_0}{\overset{\mathcal{H}_1}{\lessgtr}}\xi_{BF/GD(\hat{\sigma}_w^2)}
\end{aligned}\tag{41}$$

According to the results obtained from the proof in section V-B, the test statistic of the BF/GD under the noise power estimation scenario is expressed as:

$$\begin{aligned}
&T_{BF/GD(\hat{\sigma}_w^2)}\left(\boldsymbol{y_{bt}}\right)\\
&=(MN-2)\\
&\quad\times\frac{(N\sum_{m=1}^{M}a_m^2)\left\|\Psi+\frac{\boldsymbol{\Omega}^H\boldsymbol{w_t}(k)}{(N\sum_{m=1}^{M}a_m^2)}\right\|^2}{\|\boldsymbol{y_{bt}}\|^2-(N\sum_{m=1}^{M}a_m^2)\left\|\Psi+\frac{\boldsymbol{\Omega}^H\boldsymbol{w_t}(k)}{(N\sum_{m=1}^{M}a_m^2)}\right\|^2}\underset{\mathcal{H}_0}{\overset{\mathcal{H}_1}{\lessgtr}}\xi_{BF/GD(\hat{\sigma}_w^2)}
\end{aligned}\tag{42}$$

Logically, using the estimated value of the noise variance instead of the true value will affect the PU detection capability of the SS technique. This will be discussed later in the simulation results.

D. COMPARISON BETWEEN THE GD AND THE PROPOSED BF/GD SS TECHNIQUES

In this section, a comparison between the ULA assisted GD SS technique introduced in [10] and the proposed BF/GD technique is presented. The comparison handles their test statistics under known and unknown noise variance scenarios and the utilized techniques as listed in Table 1. Now, in case of known noise variance, we can define the improvement factor of the detection performance as:

$$\eta=\frac{\frac{(N\sum_{m=1}^{M}a_m^2)}{(\sigma_w^2/2)}\left\|\Psi+\frac{\Omega^H\boldsymbol{w_t}(k)}{(N\sum_{m=1}^{M}a_m^2)}\right\|^2}{\frac{M}{(\sigma_w^2/2)}\frac{1}{N}\left\|\sum_{n=1}^{N}\boldsymbol{y_{comb}}(n)e^{-j2\pi nf_0}\right\|^2}\tag{43}$$

where $\boldsymbol{y_{comb}}$ is the combined signal after the delay and sum beamformer. For ULA, the amplitude of the excitation coefficients of each antenna element $a_m=1\forall m=1,2,\ldots.M$. In this case, the value of the term $\sum_{m=1}^{M}a_m^2$ which appeared in the nominator of (43) equals M. However, in the proposed BF/GD SS technique, the synthesized excitation coefficients for maximum array gain realization are no longer uniform and become greater than one. Thus, the term $\sum_{m=1}^{M}a_m^2$ becomes greater than M giving improvement factor greater than one.

VI. SIMULATION RESULTS

In this section, the simulation results are divided into two main parts. The first part handles the simulation results of the proposed array beamforming technique. While the second part handles the simulation results of the proposed BF/GD SS

TABLE 1. The comparison between the GD and the proposed BF/GD SS techniques.

SS technique	Test statistic under σ_w^2	Test statistic under $\hat{\sigma}_w^2$	Utilized techniques
GD [10]	$\frac{M}{(\sigma_w^2/2)}\frac{1}{N}\left\|\sum_{n=1}^{N} \boldsymbol{y_{comb}}(n)\, e^{-j2\pi n f_0}\right\|^2$	$(MN-2)\,\frac{\frac{M}{N}\left\|\sum_{n=1}^{N} \boldsymbol{y_{comb}}(n)\, e^{-j2\pi n f_0}\right\|^2}{\sum_{m=1}^{M}\sum_{n=1}^{N}\|y_m(n)\|^2 - \frac{M}{N}\left\|\sum_{n=1}^{N} \boldsymbol{y_{comb}}(n)\, e^{-j2\pi n f_0}\right\|^2}$	1. GLRT approach. 2. Delay and sum beamforming.
Proposed BF/GD	$\frac{(N\sum_{m=1}^{M} a_m^2)}{(\sigma_w^2/2)}\left\|\Psi + \frac{\Omega^H \boldsymbol{w_t}(k)}{(N\sum_{m=1}^{M} a_m^2)}\right\|^2$	$(MN-2)\,\frac{(N\sum_{m=1}^{M} a_m^2)\left\|\Psi + \frac{\Omega^H \boldsymbol{w_t}(k)}{(N\sum_{m=1}^{M} a_m^2)}\right\|^2}{\|\boldsymbol{y_{bt}}\|^2 - (N\sum_{m=1}^{M} a_m^2)\left\|\Psi + \frac{\Omega^H \boldsymbol{w_t}(k)}{(N\sum_{m=1}^{M} a_m^2)}\right\|^2}$	1. GLRT approach. 2. Proposed antenna array beamforming. (It provides a non-uniform feeding antenna array for maximum gain realization). 3. Delay and sum beamforming.

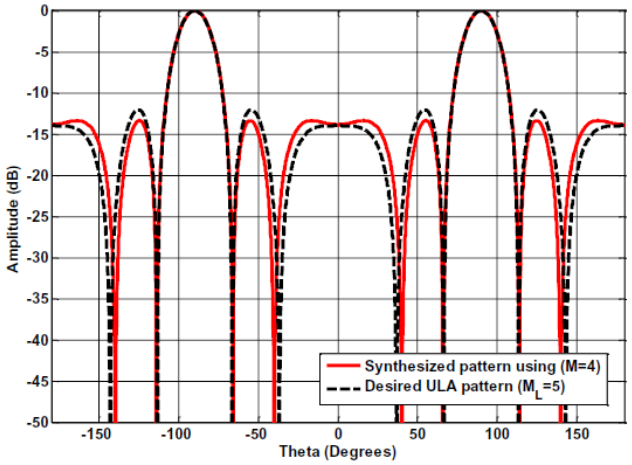

FIGURE 4. A comparison between the desired pattern of $M_L = 5$ elements ULA and the synthesized pattern using $M = 4$ elements.

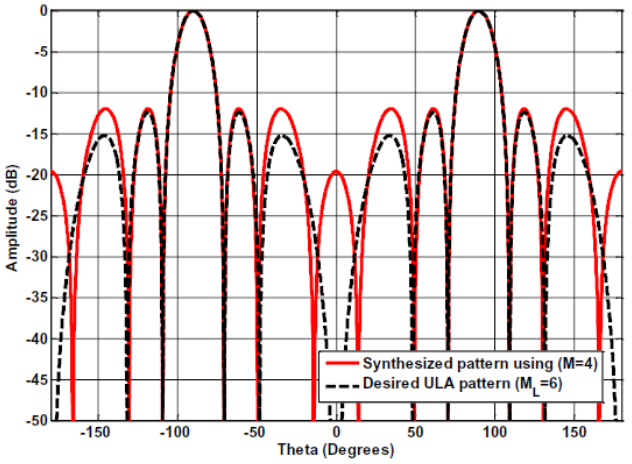

FIGURE 5. A comparison between the desired pattern of $M_L = 6$ elements ULA and the synthesized pattern using $M = 4$ elements.

technique and comparing it to other specialized algorithms in this field.

A. SIMULATION RESULTS OF THE PROPOSED ARRAY BEAMFORMING

Consider a traditional CR receiver equipped with a ULA consisting of $M = 4$ elements with uniform element spacing $d = \lambda/2$. Applying the proposed modified MoM/GA beamforming technique, the $M = 4$ elements are used to synthesize larger sized antenna arrays with different number of elements $M_L = 5, 6$, and 7. The input to the beamforming technique is the desired M_L-elements array pattern $A_{fd}(\theta)$. It determines the optimum element spacing d_b and excitation coefficients a_b required to synthesize the desired pattern. Fig. 4, Fig. 5, and Fig. 6 show comparisons between the desired and the synthesized patterns for $M_L = 5$, $M_L = 6$, and $M_L = 7$, respectively. For $M_L = 5$ and $M_L = 6$ elements, the synthesized patterns are highly matched to the desired patterns in terms of HPBW, side lobe level (SLL), and gain as shown in Fig. 4 and Fig. 5. But for $M_L = 7$, the grating

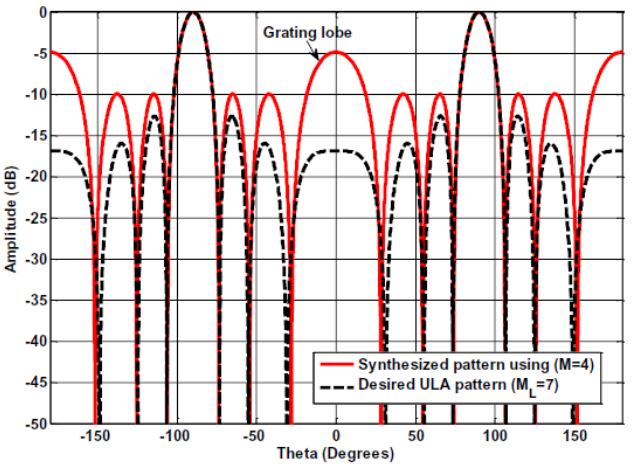

FIGURE 6. A comparison between the desired pattern of $M_L = 7$ elements ULA and the synthesized pattern using $M = 4$ elements.

lobes appear in the synthesized pattern as shown in Fig. 6. The polar plot of the synthesized array patterns compared to the 4-elements ULA pattern is shown in Fig. 7. The excitation

TABLE 2. The parameters of the synthesized antenna arrays using $M = 4$ elements for $M_L = 5, 6,$ *and* 7 elements antenna arrays compared to the traditional 4-elements ULA.

Parameters	Traditional ULA	Synthesized Array	Synthesized Array	Synthesized Array
Number of elements	$M = 4$	$M_L = 5$	$M_L = 6$	$M_L = 7$
Element spasing	$d = 0.5\lambda$	$d_b = 0.653\lambda$	$d_b = 0.768\lambda$	$d_b = 0.862\lambda$
a_1	1	1.1349	1.3933	1.2988
a_2	1	1.3479	1.4797	1.1385
a_3	1	1.3479	1.4797	1.1385
a_4	1	1.1349	1.3933	1.2988
$HPBW_d$	26.64^o	20.7^o	17.1^o	14.58^o
$HPBW_s$	26.64^o	20.7^o	17.1^o	14.58^o
SLL_d (dB)	-11.3035	-12.0412	-12.4256	-12.6522
SLL_s (dB)	-11.3035	-13.3666	-11.978	-4.8862
G_d(dB)	6.02	6.9897	7.7815	8.4510
G_s(dB)	6.02	6.9597	7.5937	6.8794
Δ_G(dB)	0	0.9397	1.5737	0.8594

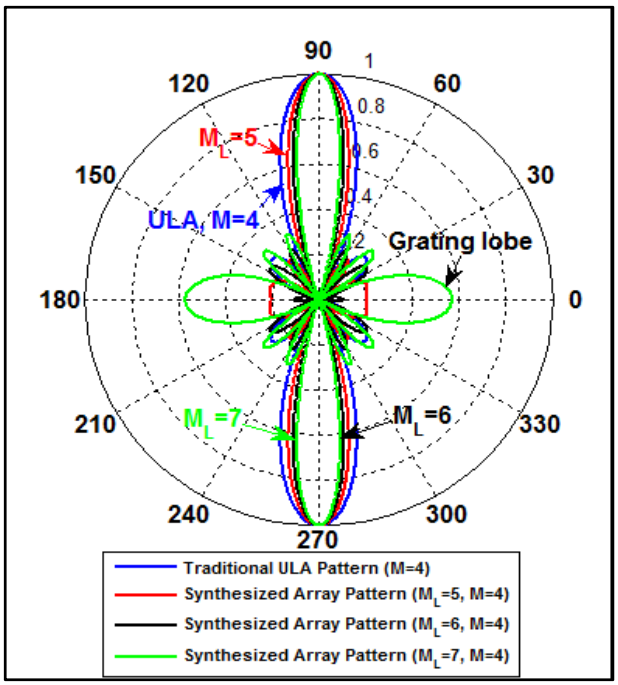

FIGURE 7. The polar plot of the synthesized arrays patterns compared to the 4-elements ULA pattern.

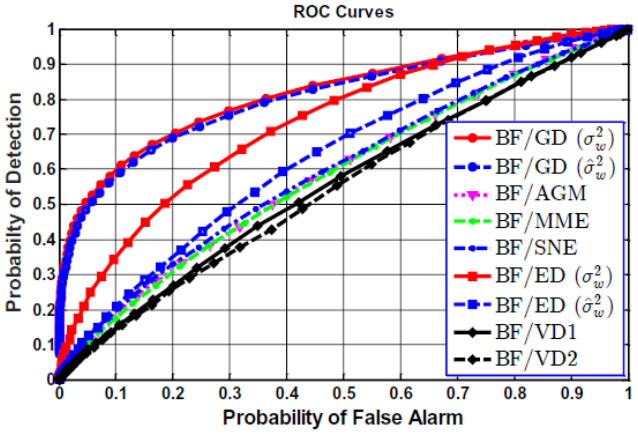

FIGURE 8. Probability of detection versus probability of false alarm for the proposed BF/GD, BF/AGM, BF/MME, BF/SNE, BF/VD1, BF/VD2, and BF/ED techniques at $M = 4$ elements, $M_L = 6$ elements, $N = 50$ samples, and $SNR = -15$dB.

TABLE 3. The estimated P_d and improvement ratio R_{P_d} for the proposed and traditional SS techniques at $M = 4$ elements, $M_L = 6$ elements, $N = 50$ samples $p_{fa} = 0.1$, and SNR $= -10$dB.

SS technique	Estimated p_d	Improvement ratio R_{P_d}%
BF/GD (σ_w^2)	0.8272	18.66
GD (σ_w^2)	0.6971	
BF/GD ($\hat{\sigma}_w^2$)	0.7983	18.66
GD ($\hat{\sigma}_w^2$)	0.6731	
BF/AGM	0.7497	161.4
AGM	0.2868	
BF/MME	0.7237	159.39
MME	0.279	
BF/SNE	0.8219	153.98
SNE	0.3236	
BF/VD1	0.5218	85.89
VD1	0.2807	
BF/VD2	0.4609	100.2
VD2	0.2302	
BF/ED (σ_w^2)	0.9113	78.54
ED (σ_w^2)	0.5104	
BF/ED ($\hat{\sigma}_w^2$)	0.5517	93.43
ED ($\hat{\sigma}_w^2$)	0.288	

coefficients, element spacing, HPBW, and SLL for the traditional 4-elements ULA and the synthesized arrays are listed in Table 2. Where, $SLL_d(dB)$ and $SLL_s(dB)$ are the desired and synthesized array side lobe levels, respectively. $G_d(dB)$ and $G_s(dB)$ are the desired and synthesized array gains, respectively. Δ_G(dB) is the realized gain increment which equals the difference between the synthesized array gain and the traditional 4-elements ULA gain.

To avoid the appearance of grating lobes and achieve the maximum gain, we chose the synthesized pattern for $M_L = 6$ elements. The synthesized gain for $M_L = 6$ elements array is $7.5937dB$ which is higher than that of the traditional 4-elements ULA by $\mathbf{\Delta}_G = 1.5937dB$. The reap reward from this gain increment will be reflected on the enhancement of the received SNR which indeed improves the SS capability of the CR receiver. Also, there is another benefit of no less important than the previous one is that the gain increment is achieved without using additional antenna elements and cost-effective RF front end chains.

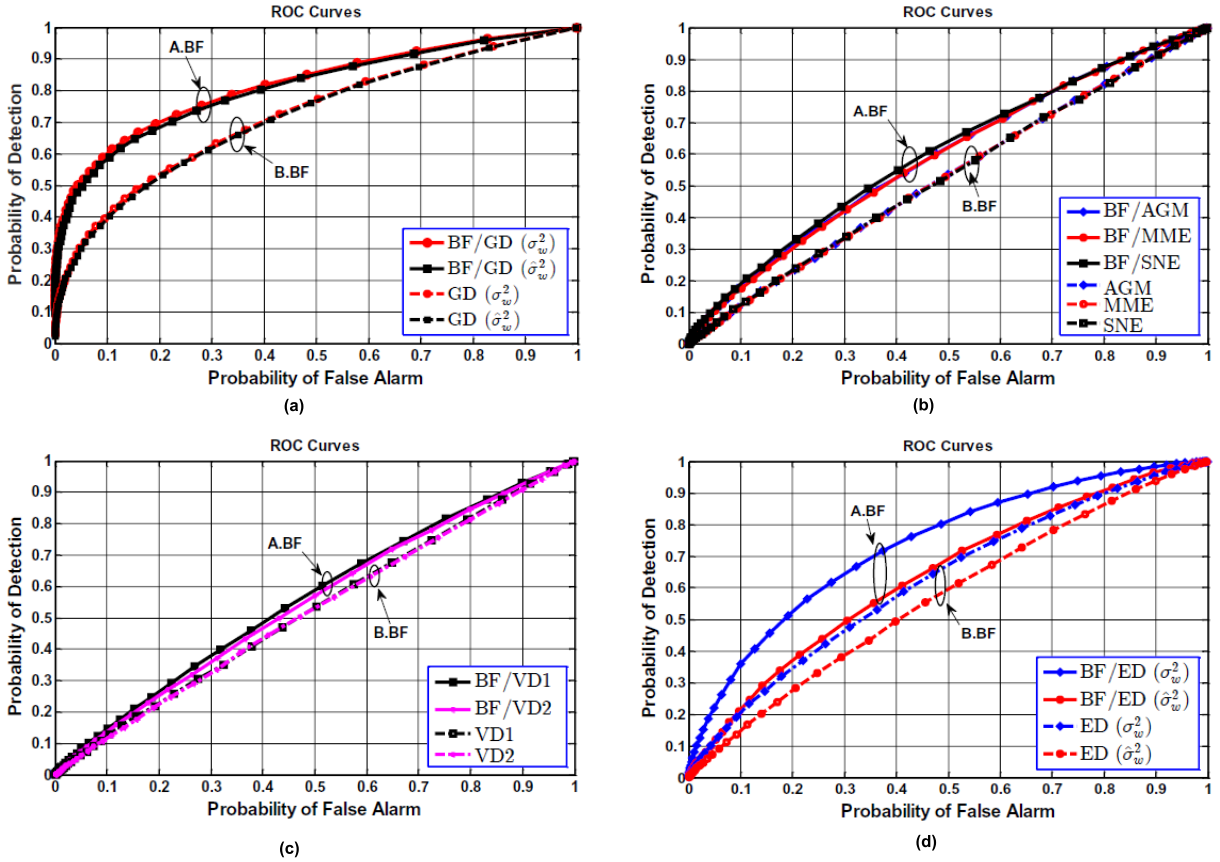

FIGURE 9. Comparison between probabilities of detection versus probabilities of false alarm before and after using the proposed array beamforming. At M = 4,M_L = 6, N = 50, andSNR = −15 dB. For: (a) GD(σ_w^2), GD($\hat{\sigma}_w^2$), BF/GD(σ_w^2), and BF/GD($\hat{\sigma}_w^2$), (b) AGM, MME, SNE, BF/AGM, BF/MME, and BF/SNE, (c) VD1, VD2, BF/VD1, and BF/VD2, (d) ED(σ_w^2), ED($\hat{\sigma}_w^2$), BF/ED(σ_w^2), and BF/ED($\hat{\sigma}_w^2$).

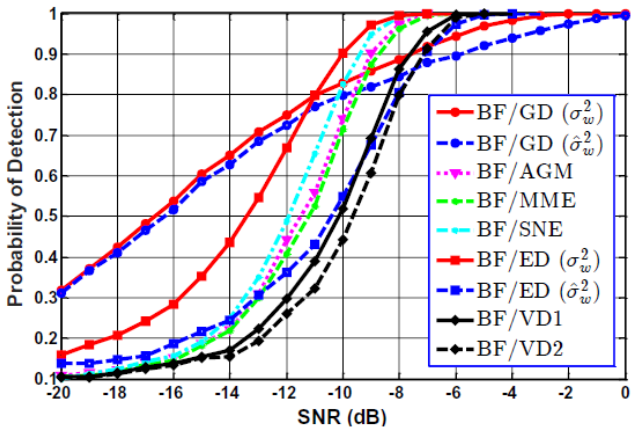

FIGURE 10. Probability of detection versus SNR for the proposed BF/GD, BF/AGM, BF/MME, BF/SNE, BF/VD1, BF/VD2, and BF/ED techniques at $M = 4$ elements, $M_L = 6$ elements, $N = 50$ samples, and $p_{fa} = 0.1$.

B. SIMULATION RESULTS OF THE PROPOSED BF/GD TECHNIQUE

In this section, several simulation scenarios were carried out to demonstrate the effect of the proposed beamforming algorithm on the performance of the most commonly used SS algorithms. It is worth mentioning that detailed analysis and derivation of the test statistic of the proposed BF/GD algorithm was introduced in the paper while the proposed beamforming based signal model is applied to AGM, MME, SNE, VD1, VD2, and ED spectrum sensing algorithms. The simulation results included the drawing of the receiver operating characteristic (ROC) curves to examine the performance of these algorithms before beamforming (B.BF) and after beamforming (A.BF). These scenarios are made considering a single PU transmitting a narrow band QPSK modulated signal. The traditional SU receiver is equipped with a ULA consisting of $M = 4$ antenna elements with uniform element spacing $d = \lambda/2$. The simulation results are averaged through 10,000 Monte-Carlo simulations.

Firstly, based on the simulation results introduced in section VI. A, it is evident that to avoid the appearance of grating lobes and achieve the maximum array gain, the $M = 4$ elements ULA is replaced by the synthesized $M_L = 6$ elements array whose parameters are listed in Table 2.

1) SCENARIO 1: PROBABILITY OF DETECTION VERSUS PROBABILITY OF FALSE ALARM

In this scenario, the probability of detection P_d versus probability of false alarm P_{fa} ROC curves are plotted for the proposed BF/GD, BF/AGM, BF/MME, BF/SNE, BF/VD1,

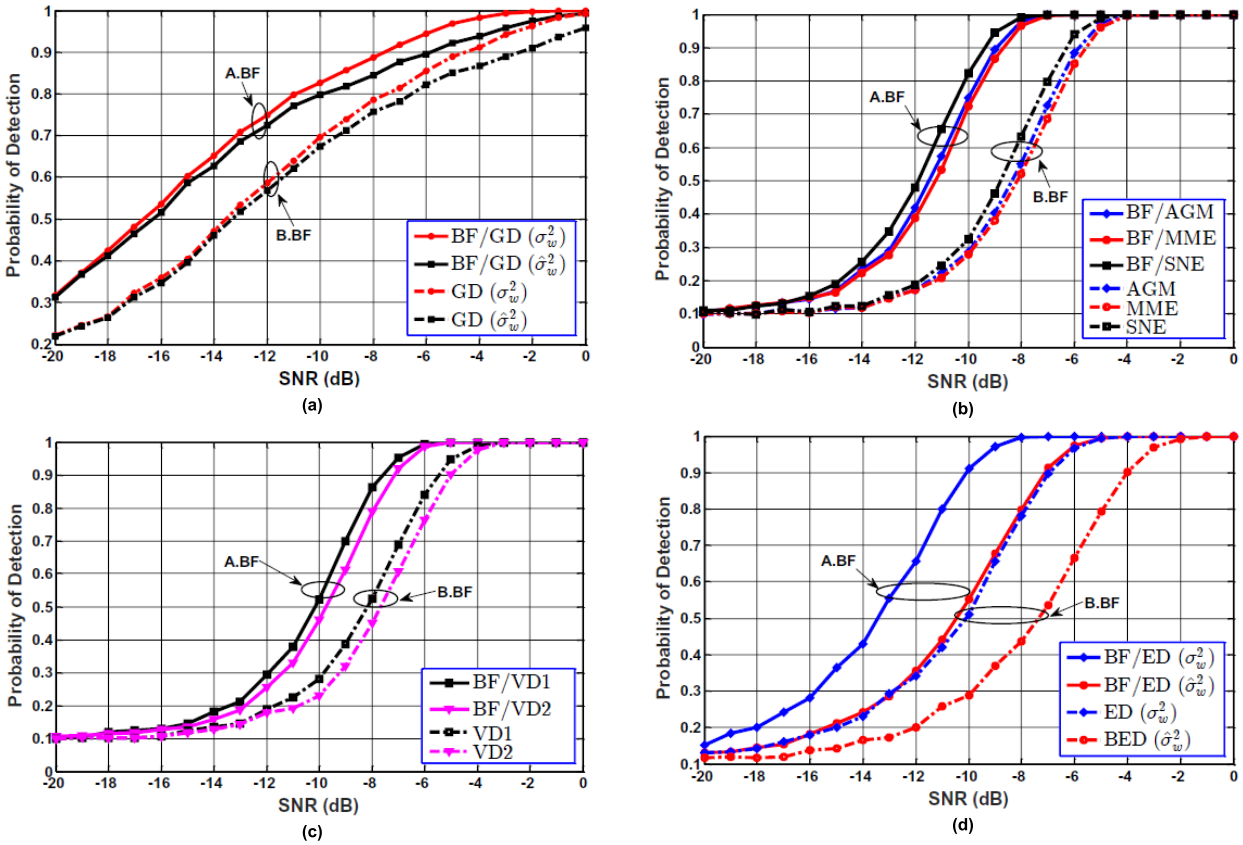

FIGURE 11. Comparison between probabilities of detection versus SNR before and after using the proposed beamforming. At M = 4 elements, M_L = 6 elements, N = 50 samples, and p_{fa} = 0.1. For: (a) GD(σ_w^2), GD($\hat{\sigma}_w^2$), BF/GD(σ_w^2), and BF/GD($\hat{\sigma}_w^2$), (b) AGM, MME, SNE, BF/AGM, BF/MME, and BF/SNE, (c) VD1, VD2, BF/VD1, and BF/VD2, (d) ED(σ_w^2), ED($\hat{\sigma}_w^2$), BF/ED(σ_w^2), and BF/ED($\hat{\sigma}_w^2$).

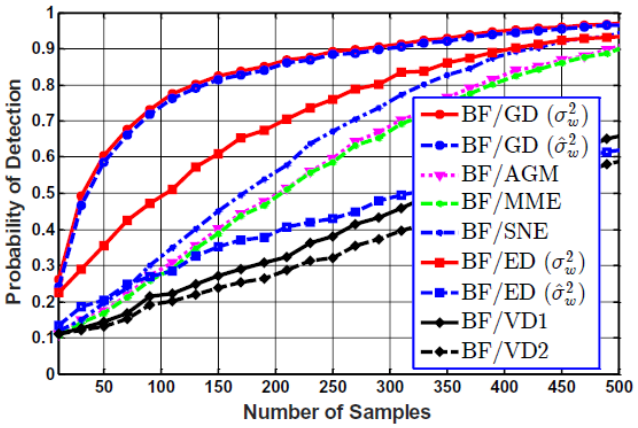

FIGURE 12. Probability of detection versus number of samples for the proposed techniques at $M = 4$ elements, $M_L = 6$ elements, $p_{fa} = 0.1$, and SNR = −15dB.

BF/VD2, and BF/ED techniques at $M = 4$ elements, $M_L = 6$ elements, $N = 50$ samples, and $SNR = -15$dB as shown in Fig. 8. While Fig. 9-(a), (b), (c), and (d) show accurate comparisons between the P_d versus P_{fa} ROC curves of the proposed techniques and traditional techniques in four separate groups to clearly distinguish the amount of improvement in performance before and after beamforming. For example, taking into account the proposed BF/GD (σ_ω^2) technique shown in Fig. (9-a) and to determine the amount of improvement in performance, we calculated the P_d at the standard $P_{fa} = 0.1$ and we found that the value of P_d is increased from 0.4 to 0.6 for the traditional and proposed techniques, respectively. It is also clear that there are noticeable outperformance and improvements in the probabilities of detection of the proposed techniques compared to the traditional techniques.

2) SCENARIO 2: PROBABILITY OF DETECTION VERSUS SNR

In this scenario, the probability of detection P_d versus SNR ROC curves are plotted for the proposed techniques at $M = 4$ elements, $M_L = 6$ elements and $N = 50$ samples, and $P_{fa} = 0.1$ over SNR range (-20dB $\leq$ SNR $\leq$ 0dB) as shown in Fig. 10. While Fig. 11-(a), (b), (c), and (d) show the P_d versus SNR ROC curves of the proposed techniques compared with the traditional techniques to demonstrate the effect of the proposed array beamforming on the detection performance of the SS techniques. To verify the superiority of the proposed techniques compared to the traditional techniques, a numerical example is taken at SNR $= -10dB$ where the corresponding probability of detections of the proposed and traditional techniques are listed in Table 3.

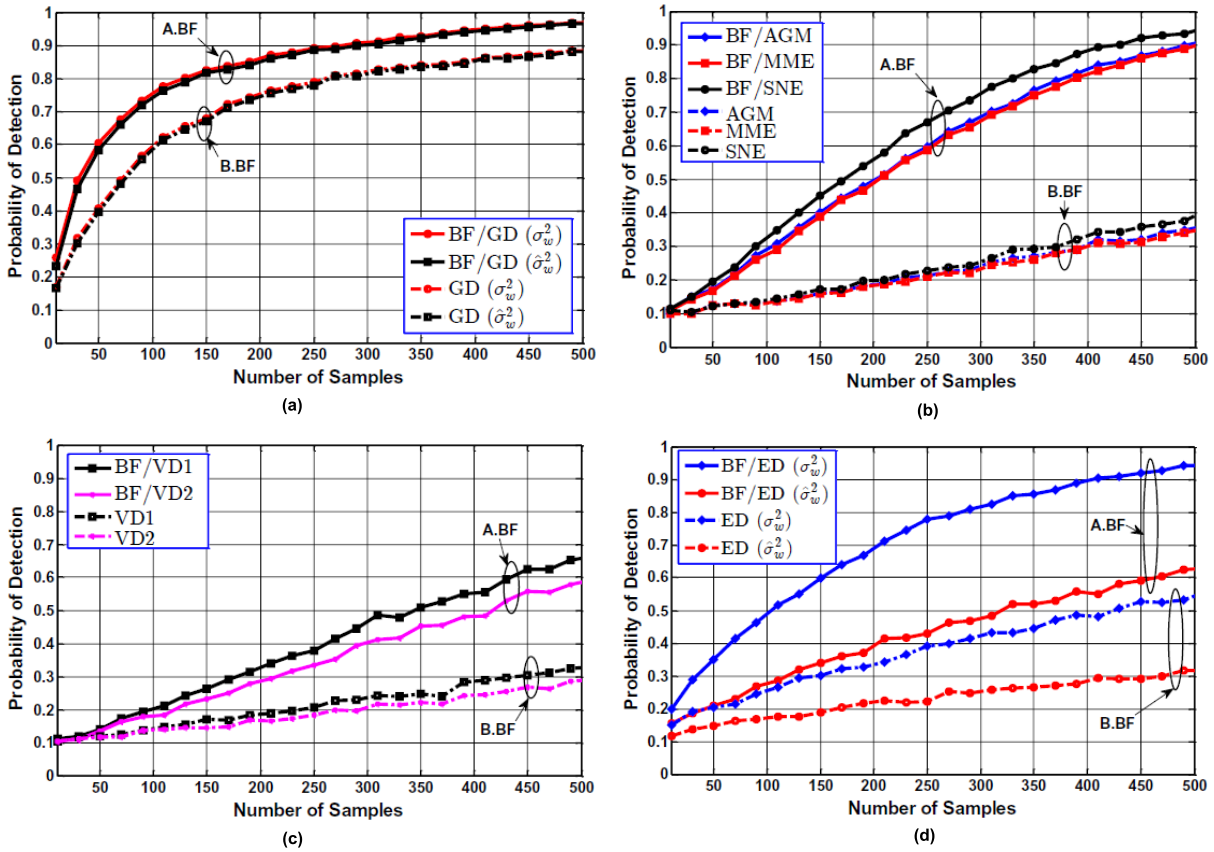

FIGURE 13. Comparison between probabilities of detection versus number of samples before and after using the proposed beamforming. At M = 4 elements, M_L = 6 elements, p_{fa} = 0.1, and SNR = −15dB. For: (a) GD(σ_w^2), GD($\hat{\sigma}_w^2$), BF/GD(σ_w^2), and BF/GD($\hat{\sigma}_w^2$), (b) AGM, MME, SNE, BF/AGM, BF/MME, and BF/SNE, (c) VD1, VD2, BF/VD1, and BF/VD2, (d) ED(σ_w^2), ED($\hat{\sigma}_w^2$), BF/ED(σ_w^2), and BF/ED($\hat{\sigma}_w^2$).

The improvement ratio in the P_d is calculated as R_{P_d}, shown at the top of the next page. From Table 3, it is evident that under the same operating conditions, the proposed techniques provide significant improvement ratios in the P_d ranging from 18.66% up to 159.39% with respect to the traditional techniques.

3) SCENARIO 3: PROBABILITY OF DETECTION VERSUS NUMBER OF SAMPLES

In this scenario, the probability of detection P_d versus number of samples N ROC curves are plotted for the proposed and traditional techniques at $M = 4$ elements, $M_L = 6$ elements, $p_{fa} = 0.1$, and SNR $= -15$dB as shown in Fig. 12. While Fig. 13-(a), (b), (c), and (d) show the P_d versus number of samples ROC curves of the proposed techniques compared with the traditional techniques. To verify the effect of the proposed array beamforming on the number of samples required to achieve the same the P_d as the traditional techniques using $N = 500$ samples at $M = 4$ elements, $M_L = 6$ elements, $p_{fa} = 0.1$, and SNR $= -15$dB, the number of samples saving ratios are calculated in Table 4 where the saving ratio R_N is calculated as follows R_N, as shown at the top of the next page. It is clear that the proposed beamforming based techniques provide significant reductions in the required number of samples ranging from 52% to 75% compared to the traditional techniques under the same operating conditions. This significant reduction in the number of received signal samples plays an effective role in reducing the required

TABLE 4. The required number of samples for the proposed techniques to achieve the same the P_d as the traditional techniques using $N = 500$ samples and the number of samples saving ratios R_N at $M = 4$ elements, $M_L = 6$ elements, $p_{fa} = 0.1$, and SNR $= -15$dB.

SS technique	Estimated p_d	Number of samples N	Saving ratio R_N%
BF/GD (σ_w^2)	0.872	230	54
GD (σ_w^2)	0.872	500	
BF/GD ($\hat{\sigma}_w^2$)	0.87	240	52
GD ($\hat{\sigma}_w^2$)	0.87	500	
BF/AGM	0.34	125	75
AGM	0.34	500	
BF/MME	0.34	130	74
MME	0.34	500	
BF/SNE	0.38	125	75
SNE	0.38	500	
BF/VD1	0.32	200	60
VD1	0.32	500	
BF/VD2	0.28	205	59
VD2	0.28	500	
BF/ED (σ_w^2)	0.54	125	75
ED (σ_w^2)	0.54	500	
BF/ED ($\hat{\sigma}_w^2$)	0.31	130	74
ED ($\hat{\sigma}_w^2$)	0.31	500	

$$R_{P_d} = \frac{P_d(after\ beamforming) - P_d(before\ beamforming)}{P_d(before\ beamforming)} \times 100$$

$$R_N = \frac{N(before\ beamforming) - N(after\ beamforming)}{N(before\ beamforming)} \times 100$$

storage space, signal processing load, system complexity, and SS time of the CR system.

VII. CONCLUSION

In this paper, highly efficient antenna arrays beamforming technique for maximum array gain realization is proposed for the application to the state-of-the-art ULA based SS techniques in CR systems. Considering the proposed beamforming the modified received signal model using the beamformed array is investigated. Along these lines, a high performance SS technique based on antenna arrays beamforming and the generalized likelihood ratio test (GLRT) denoted as BF/GD is introduced with detailed investigation of its test statistic. Furthermore, the modified received signal model is applied to the AGM, MME, SNE, VD1, VD2, and ED techniques to introduce the corresponding beamforming based BF/AGM, BF/MME, BF/SNE, BF/VD1, BF/VD2, and BF/ED techniques. The enhanced array gain significantly improved the received SNR which significantly improved the sensitivity and the SS capability of the CR receiver. The simulation results showed the superiority of the proposed techniques compared to the traditional ULA based techniques. Under the same operating conditions, the proposed techniques provide significant improvement ratios in the probability of detection ranging from 18.66% up to 159.39% with respect to the traditional techniques. Also, they provide significant reductions in the required number of samples ranging from 52% to 75% compared to the traditional techniques. It is worth noting that the application of the proposed technique to the real world is subject to further optimization according to the different application, frequency, or the array elements.

ACKNOWLEDGMENT

This work is done under the contract between the National Telecom Regulatory Authority (NTRA), Egypt, and the Electronics Research Institute in the Project entitled "Smart radar system for train collision avoidance and obstacles detection."

REFERENCES

[1] A. Goldsmith, S. Jafar, I. Maric, and S. Srinivasa, "Breaking spectrum gridlock with cognitive radios: An information theoretic perspective," *Proc. IEEE*, vol. 97, no. 5, pp. 894–914, May 2009.
[2] S. K. Sharma, S. Chatzinotas, and B. Ottersten, "Satellite cognitive communications: Interference modeling and techniques selection," in *Proc. 6th Adv. Satell. Multimedia Syst. Conf. (ASMS) 12th Signal Process. Space Commun. Workshop (SPSC)*, Sep. 2012, pp. 111–118.
[3] I. F. Akyildiz, W.-Y. Lee, M. C. Vuran, and S. Mohanty, "Next generation/dynamic spectrum access/cognitive radio wireless networks: A survey," *Comput. Netw.*, vol. 50, no. 13, pp. 2127–2159, Sep. 2006.
[4] A. Mariani, A. Giorgetti, and M. Chiani, "Effects of noise power estimation on energy detection for cognitive radio applications," *IEEE Trans. Commun.*, vol. 59, no. 12, pp. 3410–3420, Dec. 2011.
[5] M. López-Benítez and F. Casadevall, "Improved energy detection spectrum sensing for cognitive radio," *IET Commun.*, vol. 6, no. 8, p. 785, 2012.
[6] Y. Zeng and Y.-C. Liang, "Eigenvalue-based spectrum sensing algorithms for cognitive radio," *IEEE Trans. Commun.*, vol. 57, no. 6, pp. 1784–1793, Jun. 2009.
[7] R. Zhang, T. Lim, Y.-C. Liang, and Y. Zeng, "Multi-antenna based spectrum sensing for cognitive radios: A GLRT approach," *IEEE Trans. Commun.*, vol. 58, no. 1, pp. 84–88, Jan. 2010.
[8] A. Taherpour, M. Nasiri-Kenari, and S. Gazor, "Multiple antenna spectrum sensing in cognitive radios," *IEEE Trans. Wireless Commun.*, vol. 9, no. 2, pp. 814–823, Feb. 2010.
[9] L. Huang, H. So, and C. Qian, "Volume-based method for spectrum sensing," *Digit. Signal Process.*, vol. 28, pp. 48–56, May 2014.
[10] H. S. Fouda, A. H. Hussein, and M. A. Attia, "Efficient GLRT/DOA spectrum sensing algorithm for single primary user detection in cognitive radio systems," *AEU-Int. J. Electron. Commun.*, vol. 88, pp. 98–109, May 2018.
[11] P. Barton, "Digital beamforming for radar," *IEE Proc. F Radar Signal Process.*, vol. 127, pp. 266–277, Aug. 1980.
[12] E. Brookner, "Trends in array radars for the 1980's and beyond," *IEEE Antennas Propag. Soc. Newslett.*, vol. APSN-26, no. 2, pp. 27–30, Apr. 1984.
[13] H. Steyskal, "Digital beamforming antennas—An introduction," *Microw. J.*, vol. 30, pp. 107–124, Jan. 1987.
[14] Y. Liu, Z. Nie, and Q. H. Liu, "Reducing the number of elements in a linear antenna array by the matrix pencil method," *IEEE Trans. Antennas Propag.*, vol. 56, no. 9, pp. 2955–2962, Sep. 2008.
[15] Y. Liu, Q. H. Liu, and Z. Nie, "Reducing the number of elements in the synthesis of shaped-beam patterns by the forward-backward matrix pencil method," *IEEE Trans. Antennas Propag.*, vol. 58, no. 2, pp. 604–608, Feb. 2010.
[16] D. Kurup, M. Himdi, and A. Rydberg, "Synthesis of uniform amplitude unequally spaced antenna arrays using the differential evolution algorithm," *IEEE Trans. Antennas Propag.*, vol. 51, no. 9, pp. 2210–2217, Sep. 2003.
[17] S. Ho and S. Yang, "Multiobjective synthesis of antenna arrays using a vector tabu search algorithm," *IEEE Antennas Wireless Propag. Lett.*, vol. 8, pp. 947–950, 2009.
[18] V. Murino, A. Trucco, and C. Regazzoni, "Synthesis of unequally spaced arrays by simulated annealing," *IEEE Trans. Signal Process.*, vol. 44, no. 1, pp. 119–122, Jan. 1996.
[19] K. Chen, X. Yun, Z. He, and C. Han, "Synthesis of sparse planar arrays using modified real genetic algorithm," *IEEE Trans. Antennas Propag.*, vol. 55, no. 4, pp. 1067–1073, Apr. 2007.
[20] N. Jin and Y. Rahmat-Samii, "Advances in particle swarm optimization for antenna designs: Real-number, binary, single-objective and multiobjective implementations," *IEEE Trans. Antennas Propag.*, vol. 55, no. 3, pp. 556–567, Mar. 2007.
[21] A. H. Hussein, H. H. Abdullah, A. M. Salem, S. Khamis, and M. Nasr, "Optimum design of linear antenna arrays using a hybrid MoM/GA algorithm," *IEEE Antennas Wireless Propag. Lett.*, vol. 10, pp. 1232–1235, 2011.
[22] E. Basma, H. H. Amr, H. A. Haythem, and S. Khamis, "Synthesis of pencil beam linear antenna arrays using simple FFT/CF/GA based technique," *Int. J. Eng. Technol.*, vol. 13, no. 5, pp. 1–5, 2013.
[23] W. Shi, Y. Li, L. Zhao, and X. Liu, "Controllable sparse antenna array for adaptive beamforming," *IEEE Access*, vol. 7, pp. 6412–6423, 2019.
[24] J. F. de Andrade, M. L. R. de Campos, and J. A. Apolinário, "L_1 -constrained normalized LMS algorithms for adaptive beamforming," *IEEE Trans. Signal Process.*, vol. 63, no. 24, pp. 6524–6539, Dec., 2015.
[25] X. Zhang, T. Jiang, Y. Li, and Y. Zakharov, "A novel block sparse reconstruction method for DOA estimation with unknown mutual coupling," *IEEE Commun. Lett.*, vol. 23, no. 10, pp. 1845–1848, Oct. 2019.
[26] S. M. Kay, *Fundamentals of Statistical Signal Processing: Detection Theory*, vol. 2. Upper Saddle River, NJ, USA: Prentice-Hall, 1998.

AMR HUSSEIN HUSSEIN received the B.Sc. degree in electronics and electrical communications engineering from Tanta University, Egypt, in 2001, and the M.Sc. and Ph.D. degrees from Tanta University, in 2007 and 2012, respectively. He was an Associate Professor with Tanta University, in 2017. His M.Sc. degree is dedicated to the VHDL implementation of both multiple access interference (MAI), and Inter-symbol interference (ISI) cancellers for DS-CDMA communications using field-programmable gate arrays (FPGAs). The Ph.D. degree is devoted to introducing new MoM/GA-based algorithms for different digital beamforming applications which are of main concern in the recent and future wireless communication systems. He has also introduced VHDL implementations of both DOA estimation algorithms and the fixed beamwidth electronic scanning (FBWES) algorithm.

HAGER SHAWKY FOUDA received the B.Sc. and M.Sc. degrees in electronics and electrical communications engineering from Tanta University, Egypt, in 2011 and 2018, respectively. She is interested in signal processing algorithms.

HAYTHEM HUSSEIN ABDULLAH received the B.Sc. degree in electronics and communication engineering from the University of Benha, Egypt, in 1998, and the M.Sc. and Ph.D. degrees from Cairo University, in 2003 and 2010, respectively. His M.Sc. degree is dedicated in the simulation of the dispersive materials in the Finite Difference Time Domain numerical technique and its application to the SAR calculations within the human head. The Ph.D. degree is dedicated to the radar target identification. He is currently an Associate Professor and the Head of the Nanotechnology Laboratory, Electronics Research Institute (ERI), Cairo, Egypt. His current research interests are design and optimization of microstrip antenna arrays and their applications. He was PI of two projects funded from different funding agencies. He has participated in 13 research projects at the national and international levels under the Egypt–NSF–USA joint funds program, the NTRA, STDF, and the National Authority of Remote Sensing.

ASHRAF A. M. KHALAF received the B.Sc. and M.Sc. degrees in electrical engineering from Minia University, Egypt, in 1989 and 1994, respectively, and the Ph.D. degree in electrical engineering from the Graduate School of Natural Science and Technology, Kanazawa University, Japan, in March 2000. He is currently an Associate Professor with the Electronics and Communications Engineering Department, Faculty of Engineering, Minia University, Egypt.